Instrumentation Science & Technology
Publication details, including instructions for authors and subscription information:
http://www.tandfonline.com/loi/list20

DESIGN OF AN AUTOMATED FEEDBACK CONTROL COOLING SYSTEM FOR SWIR LINEAR IMAGE SENSOR APPLICATION

Chien-Hung Chen [a], Chih-Wen Chen [a], Chun-Fu Lin [a b], Tai-Shan Liao [a], Chi-Hung Hwang [a] & Shir-Kuan Lin [b]

[a] Instrument Technology Research Center, National Applied Research Laboratories, Hsinchu, Taiwan, Republic of China

[b] Institute of Electrical Control Engineering, National Chiao Tung University, Hsinchu, Taiwan, Republic of China

Published online: 21 Apr 2010.

To cite this article: Chien-Hung Chen, Chih-Wen Chen, Chun-Fu Lin, Tai-Shan Liao, Chi-Hung Hwang & Shir-Kuan Lin (2010) DESIGN OF AN AUTOMATED FEEDBACK CONTROL COOLING SYSTEM FOR SWIR LINEAR IMAGE SENSOR APPLICATION, Instrumentation Science & Technology, 38:3, 234-246, DOI: 10.1080/10739141003707840

To link to this article: http://dx.doi.org/10.1080/10739141003707840

Instrumentation Science and Technology, 38:234–246, 2010

ISSN: 1073-9149 print/1525-6030 online
DOI: 10.1080/10739141003707840

Taylor & Francis
Taylor & Francis Group

DESIGN OF AN AUTOMATED FEEDBACK CONTROL COOLING SYSTEM FOR SWIR LINEAR IMAGE SENSOR APPLICATION

Chien-Hung Chen,[1] Chih-Wen Chen,[1] Chun-Fu Lin,[1,2] Tai-Shan Liao,[1] Chi-Hung Hwang,[1] and Shir-Kuan Lin[2]
[1]*Instrument Technology Research Center, National Applied Research Laboratories, Hsinchu, Taiwan, Republic of China*
[2]*Institute of Electrical Control Engineering, National Chiao Tung University, Hsinchu, Taiwan, Republic of China*

☐ *Our novel automated feedback temperature controlled cooling system consists of a temperature measurement circuit, a TE cooler, a thermistor, a microcontroller, and a digital-to-analog converter and PWM algorithms. The measurement accuracy of this temperature controlled TE system was better than 0.1°C and can be used for maintaining an instrument's isothermal applications. The experimental results of SWIR linear image shows that the temperature can be stably maintained at −20°C, the dark output current can be reduced almost 80 mV (Integration time: 100 ms) and the SNR of pixel can be improved from 48 dB to 83 dB as well.*

Keywords automated feedback, PWM, SNR, SWIR linear image, TE cooler, temperature control

INTRODUCTION

An isothermal environment is an essential requirement for accurate instruments to perform delicate, precise, and accurate measurements. Currently, instruments are always required to operate with high data acquisition rates and high measurement accuracies. However, instruments operated with high data acquisition rates always encounter current conducted heat, and rising temperatures become a problem. If generated waste heat cannot be properly dispersed and dissipated by thermal control units or devices, instruments operated in high temperature environments could produce drifts in measured data or even failures in overall data acquisition. Therefore, controlling the operation temperature for instruments has two

Address correspondence to Chien-Hung Chen, Instrument Technology Research Center, National Applied Research Laboratories, 20 R&D Rd VI, Hsinchu Science Park, Hsinchu, 300, Taiwan, R.O.C. E-mail: cchung@itrc.org.tw

advantages. The first advantage is the improvement of the SNR range of the measurement,[1] and the second is the extension of the lift-cycle of an instrument's components. Cooling methods such as those involving thermoelectric (TE) coolers, helium liquefier refrigeration, and nitrogen liquid refrigeration are widely applied to control instrument operation temperatures. Both helium liquefier and nitrogen liquid refrigeration methods are capable of cooling the temperature down to several Kelvin and maintaining these lower temperatures. However, helium liquefier and nitrogen liquid refrigeration require complex and expensive supporting systems.

The application of helium liquefier and nitrogen liquid refrigeration is suitable for large imaging sensors such as cameras used in astronomy because of the heavy investment.

The TE cooling device has attracted attention for portable instrumental applications because the TE cooling device is of simple construction and small in size. Another advantage of a TE cooling device is the fact that the associated cooling control module can easily be integrated into the circuits of an instrument. This easy integration is why TE cooling devices are widely used in many applications.[2,3] The most important application of the TE cooling device is its usage in high performance imaging sensors because every 10°C temperature increase in the image sensor yields an order of high noise voltage output.

A TE cooling module consists of several N & P pellets connected electrically in series and arranged thermally in parallel while sandwiched between two ceramic plates as shown in Figure 1. The sandwich structure performs endothermically at the left hand side substrate and exothermically at the right hand side substrate when the electric current flows from an n-type semiconductor to a p-type semiconductor. If the current polarity is switched, the cold and hot surfaces are also switched. The performance

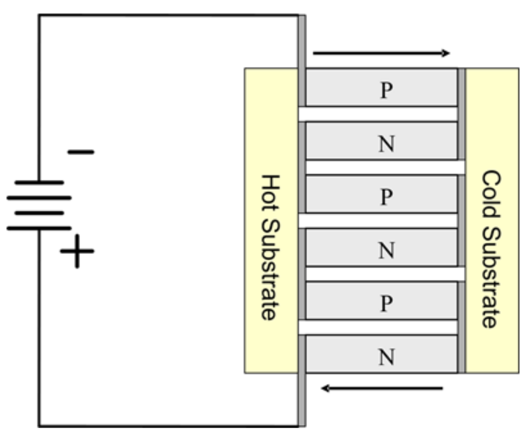

FIGURE 1 TE cooling module.

of the TE cooling depends on the temperature difference (ΔT) between the cold surface and the hot surface. Physically, the ΔT of the TE module is determined by the stacking numbers of the n-type and p-type semiconductor pellets and the operation current. Currently, TE cooling designs are focused on the improvement of the TE module and the mechanism of the exothermic reaction of the TE cooler[4,5] or measurement method,[6] but only a few researchers work on the TE cooling control method. However, the temperature difference ΔT between the cold surface and the hot surface is a key parameter to in TE cooling, and hence, maintaining a low temperature at the hot surface will allow the cold surface temperature to become even colder.

A good control method would allow a TE cooling module to achieve the greatest benefit. The general method of TE cooling control uses transistors to switch current to reduce the temperature.[7,8] This kind of method must modulate the current output very carefully as the large, transient current output might damage the instrument. Another way to control the current output is to use Pulse-Width Modulation (PWM) signals. The pulse width of PWM signals can affect the time of the transistor switch. Therefore, the different duty cycle of PWM signals will control the current output. In this paper, a TE cooling control system utilizing PWM algorithms provides a current control and automatic temperature feedback control function. After the user sets the cooling temperature, the temperature sensor circuits, which we included in this design, measure the TE cooling temperature, and the system automatically controls the PWM signals to modify the current output. One dark signal output of the image sensor experiment successfully confirmed the system function based on the PWM algorithm. The magnitude of the electronic noise and dark current of the sensor are major parameters concerning the quality of an image sensor. Detailed information is lost when the dark state output becomes too large. On the other hand, a lower output of the dark state can also provide a high SNR signal and a wider dynamical range of the sensor output.[9] Since both the dark current and the circuit noise of the sensors increase as temperature increases, maintaining the sensors at low temperatures becomes an important issue. Thereby, we used the dark signal output of our short wave infrared (SWIR) linear image sensor experiment to verify this system performance and found the relationship between temperature and dark signal output of the image sensor.

TE COOLING SYSTEM CIRCUIT

Figure 2 shows the circuit diagram of the TE cooling system. The main blocks of this design are the temperature measurement circuit, digital-to-analog

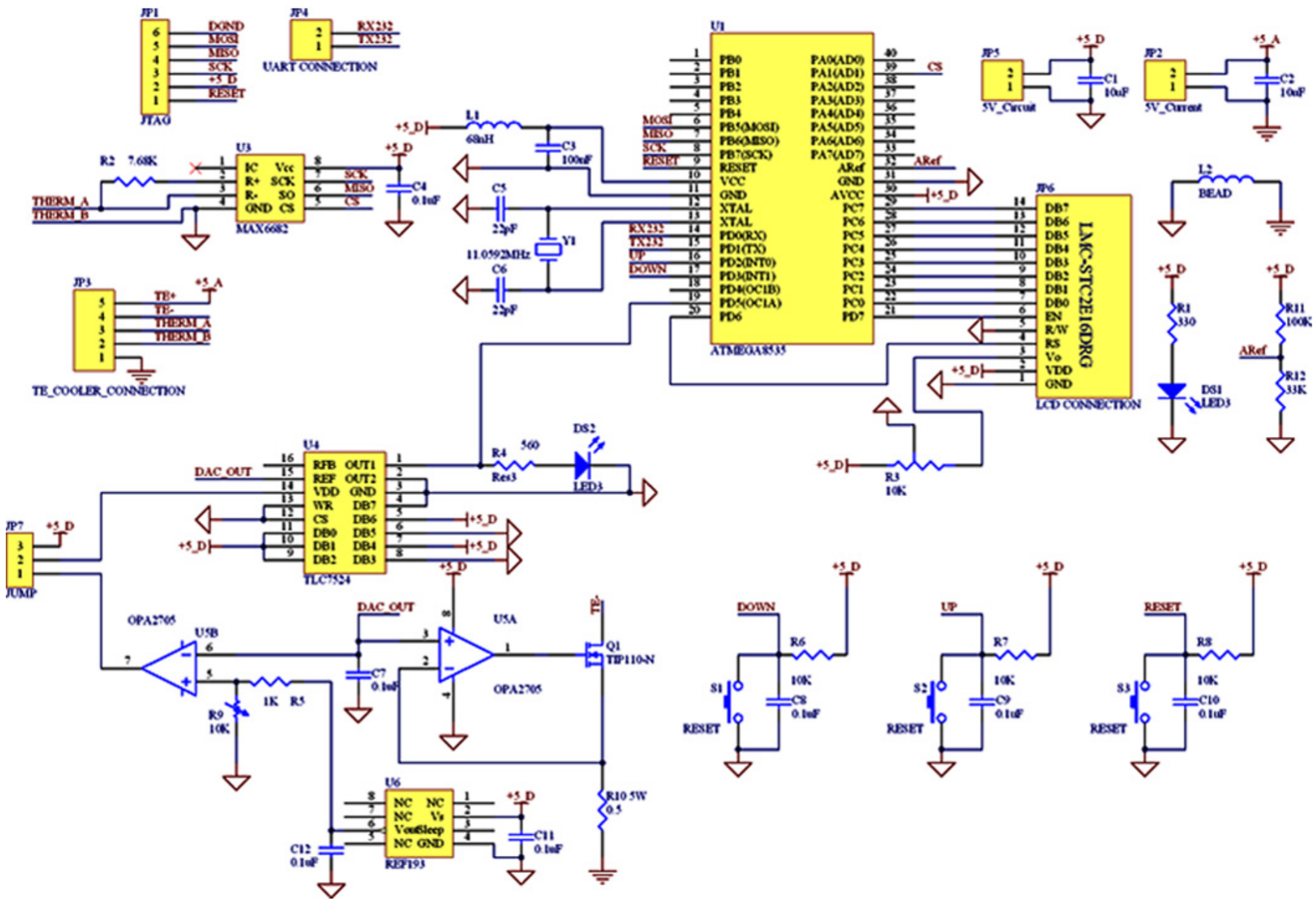

FIGURE 2 Complete circuit diagram of the TE cooling system.

converter (DAC), current output circuit, safeguard circuit, and liquid crystal display (LCD). This system can read the temperature parameters from different types of temperature sensors.

The thermistor's circuit included a thermistor-to-digital converter (U3 in Figure 2, MAX6682, Maxim) and microcontroller (U1 in Figure 2, ATMEGA8535, Atmel[10]). The thermistor-to-digital converter produced the negative temperature coefficient (NTC) thermistor and generated digital signals from the analog temperature signal. The thermistor-to-digital converter could generate a constant current for the fixed resistance (R2 in Figure 2, 7.68 k) and the thermistor's temperature dependent resistance of the device, which interfaced to JP3 THERM_A and THERM_B. When the current passed through the fixed resistor and the temperature altered the thermistor resistance, the voltage was measured and directly converted into a digital format. The thermistor-to-digital converter interfaced with the microcontroller via a 3-wire Serial Peripheral Interface (SPI)-compatible interface (SCK, MISO, and CS in Figure 2). The SPI module, which included the microcontroller, received the temperature data in master operation (PB5, PB6, and PB7 in Figure 2). Another temperature sensor processed the seat back effect and provided a voltage signal when the circuit of this type of temperature sensor was simpler than the thermistor circuit. It included a microcontroller and resistances (R11, R12, and R13 in Figure 2). The microcontroller was embedded in a 10-bit successive approximation analog-to-digital converter. The voltage that will be changed by temperature could be input into the single-ended voltage from the pin of PA0. The single-ended voltage inputs referred to 0 V (GND). The minimum value of ADC represented the GND, and the maximum value of ADC represented the output voltage of the AREF pin minus 1 LSB. Therefore, those resistors (R11, R12, and R13) were designed to modify the maximum value and change the input range of the ADC. It could also select AVCC or an internal 2.56 V reference voltage by writing to the REFSn bits in the microcontroller ADMUX Register.

In the current output, we compared two methods. These methods were simple I/O control and the Pulse-Width Modulation (PWM) control. They both used the same circuits, which included the DAC (TLC7524), Operational Amplifiers (OPA, OPA2705), and the MOSFET. Both I/O control and PWM control could be selected by the PD5 pin of the microcontroller and then input into the DAC. TLC7524 is one type of digital-to-analog converter (DAC), which is designed to easily interface with the most popular microprocessors. We applied a fixed voltage from the microcontroller to the current output terminal (U4, pin 1 in Figure 2). The analog output voltage was then available at the reference voltage terminal (U4, pin 15 in Figure 2). The relationship of both the fixed input voltage and the analog output voltage is given by the following equation: $VO = VI\ (D/256)$, where VO is the analog output voltage, VI is the fixed input voltage, and D is the digital input code converted to a decimal. In this design, the digital input was fixed for the same voltage output (U4, pins 4–11 in Figure 2). The DAC output voltage was sent to the driver circuits, which included an OPA (U5A) and an N-channel MOSFET (Q1, TIP110 in Figure 2).

The MOSFET turned on as the gate of the MOSFET was activated. The current passed through both the Pin TE+ and TE− and then on to R10. On other hand, we also designed a safeguard circuit in this project. It included an OPA (U5B) and reference voltage IC (REF193). The reference IC could provide a stable 3 V voltage. We constructed the OPA (U5B) and resistance R5 and R9 as a comparator circuit. Based on Ohm's Law, we could modify the R9 to change the V+ voltage of the OPA (U5B). DAC output also interfaced to the V− voltage of the OPA (U5B). When the DAC output voltage was more than the V+ voltage of the OPA (U5B), this OPA output a low voltage (GND). Therefore, the JP7 could be used to switch the safeguard function on and off.

To display the temperature setting of the cooling function and the automatic feedback temperature data, we designed an LCD in this circuit. The LCD was interfaced with the microcontroller by eight data lines and two control lines (PB0–7, PD6, and PD7 in Figure 2). We could also set and measure the temperature setting of the cooling function and the feedback temperature data via the URTA interface (JP4 in Figure 2). The control software was written in KEIL C IDE for the operation of the TE cooling system, including such functions as setting the SPI interface to read the temperature data of the thermistor circuit from the thermistor-to-digital converter or embedded ADC function. The program then converted the temperature into degrees Celsius and provided PWM feedback signals for the current output. The TE cooling device needed to have a larger operating current to cause a temperature difference on the TE cooling surface. Therefore, this TE cooling system required two independent 5 V DC power supplies for the system circuit and the TE cooling device.

Figure 3 shows the flowchart of the program loaded in the microcontroller. There were several parameters that needed to be initiated, including the analog, digital, SPI, and PWM functions of the microcontroller as well as the registers of Timer 1. Thus, the control software enabled Timer 1 and set the anticipated cooling temperature. We set the initial anticipated cooling temperature to 20°C. During all the process, the anticipated cooling temperature could be updated. After those parameters initialized, the temperature was repeatedly measured by the thermistor and displayed on the LCD. The Timer function calculated the difference in temperature from the measurement temperature data and the anticipated cooling temperature. If the measured temperature was greater than the anticipated cooling temperature, the microcontroller increased the duty cycle of the

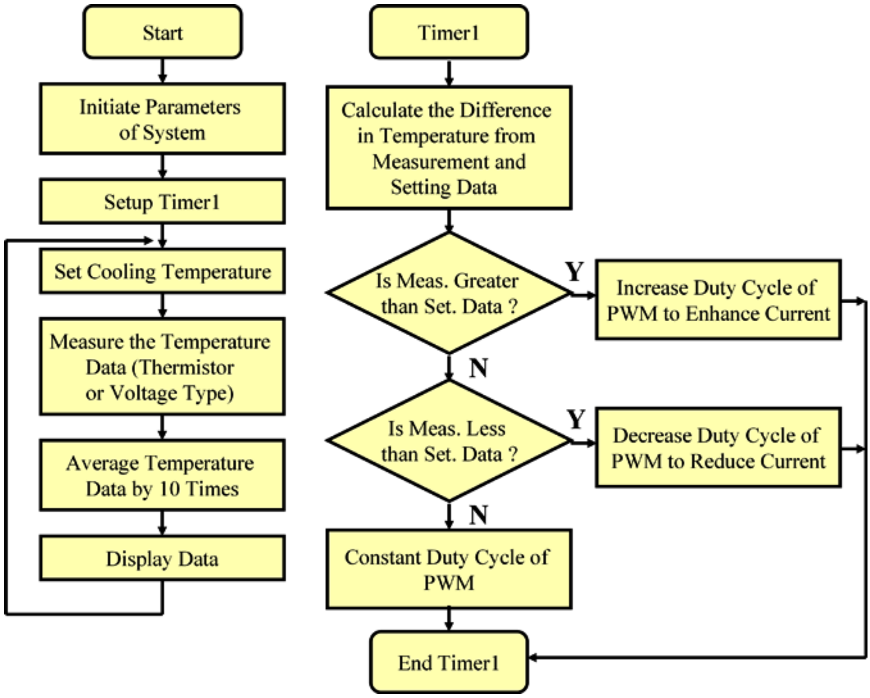

FIGURE 3 Flowchart of the TE cooling system program.

PWM signal to enhance the current to the TE cooling module. If the measured temperature was less than the anticipated cooling temperature, then the microcontroller decreased the duty cycle of the PWM signal to reduce the current. However, if the measured temperature was the same as the anticipated cooling temperature, the microcontroller maintained the duty cycle of the PWM signal and current. All of the data updated constantly and was displayed on the LCD.

We built an experiment to test the TE cooling system. In the experiment, the SWIR InGaAs linear image sensor (G9201-256S, Hamamatsu[11]) was used to verify the performance of the TE cooling system. During the experiment, it tested the performance of our cooling system and studied the effects of integrating time and temperature with the dark state output of the SWIR sensor. Figure 4 shows the flowchart of the experiment. These parameters were initialized before the experiment began. They included the output current of the controller, which was set to 0 A. The integration time of the image sensor was set to about 1 ms, and the SWIR sensor was completely covered during the experiments. The thermistor embedded in the InGaAs image sensor provided temperature data. Therefore, the cooling system measured the temperature via the thermistor-to-digital

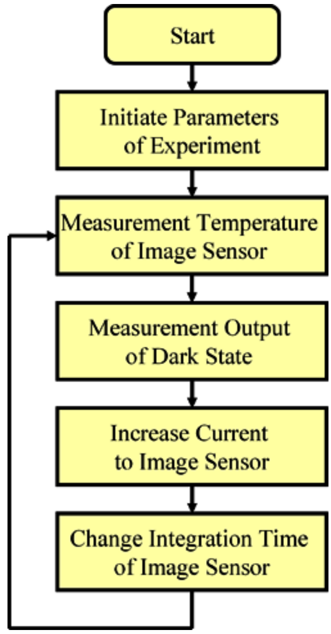

FIGURE 4 Flowchart of the experiment of the TE cooling system testing.

converter. The temperature data of the image sensor and the output of the dark state were monitored first. Then, we increased the current input to the image sensor and changed the integration time. The data from the image sensor was recorded when integration times were 1 ms, 10 ms, 50 ms, 75 ms, and 100 ms at different input currents of the TE cooler of 0 A, 0.5 A, 1 A, 1.5 A, and 2 A, respectively. We also used all pixel output standard deviation values to analyze the output stability.

RESULTS AND DISCUSSION

We fabricated our TE cooling system on a small printed circuit board (PCB) along with passive surface mount device components. The PCB was 8×4.5 cm. Figure 5 shows the different thermistor values converted to a temperature curve by the thermistor-to-digital converter. The minimum and maximum thermistor values (R) measured with the thermistor sensor were about 1 k and 35 k, respectively. We obtained thermistor values over a measured range from 80°C to −20°C.

Figure 6 shows the different voltage sensor output values converted to a temperature curve. The dynamic range of the ADC input, which was embedded on the microcontroller, was dependent on the input voltage

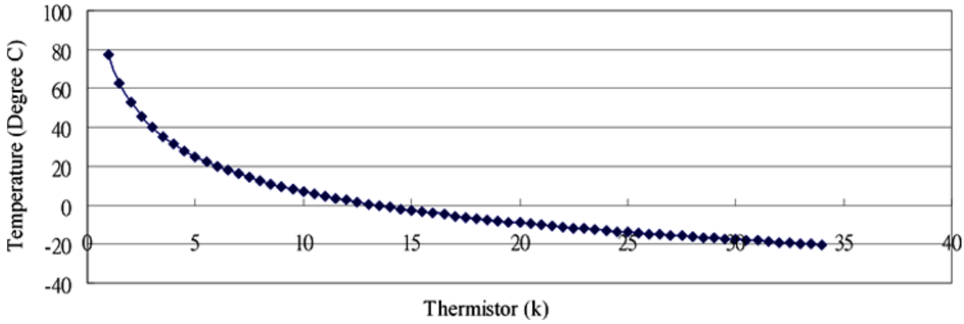

FIGURE 5 Thermistor to temperature data.

of the AREF pin. In the test, the AREF pin voltage was 1.1 V. Therefore, all the dynamic range could be converted from 0 V to 1.1 V. The 10-bit converter's resolution was about 0.001 V, which was given by the following equation: Res. = dynamic range/1024.

The advantages of the temperature measurement of the thermistor were that it could transfer the temperature data via the resistance of the thermistor without supplying power and that it was easy to use. However, the thermistor needed other circuits that included a thermistor-to-digital converter function to convert temperature data like the MAX6682 IC in this research. On the other hand, the data of the temperature measurements of the voltage type could be easily converted by the microcontroller, which included the ADC function. The disadvantage of the voltage type was that it required power to convert the temperature data to a voltage. The resolution of the temperature measurement of the thermistor type was also about 0.1°C. In the current output of the TE controller, we compared these two methods that included simple I/O and PWM control. First, we tested simple I/O control. When the I/O (PD5 in Figure 2) level was high, the output of the DAC was about 2.73 V to the OPA and the base of the NPN transistor (TIP110). The high supply current could pass through the

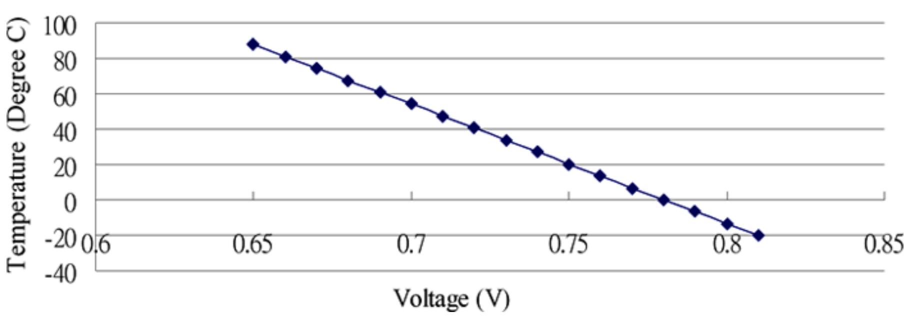

FIGURE 6 Voltage to temperature data.

collector and the emitter of the NPN transistor to the device. Under these conditions, the NPN transistor was operating in the saturation region. The other method to control current output was through PWM signals. The pin PD5 of the microcontroller could generate PWM signals to the DAC. Then, the DAC output voltage directly transferred to the OPA and NPN transistor (TIP110).

Figure 7 shows the relationship between the pulse width of the PWM signals and the DAC output voltage as well as the output current. With the simple I/O method, when the transistor was open, the whole current was applied to the TE device. This behavior could cause damage to the TE device. In the PWM method, the NPN transistor was operating in the linear region. The different voltage was output from the DAC by a different pulse width of the PWM signal because of the included capacitance of the DAC. The DAC voltage was higher because of the high duty ratio pulse width of the PWM and output to the base of the NPN transistor. When the base voltage of the NPN transistor increased, the current path through the collector and the emitter of the NPN transistor was also enhanced. Therefore, the PWM method could be easily used to control the current value. In this research, we integrated the PWM method of current control and the temperature measurement of the thermistor to experiment on the dark output of the InGaAs image sensor.

We also used the TE cooling system presented in this paper to cool the SWIR InGaAs image sensor. Figure 8 shows the relationship of driving the current of the TE cooler and the temperature of the image sensor. The thermistor, which was embedded in the SWIR image sensor, measured the its temperature data. The anticipated cooling temperature was be set by user. The temperature data feedback signal automatically modulated the PWM signal.

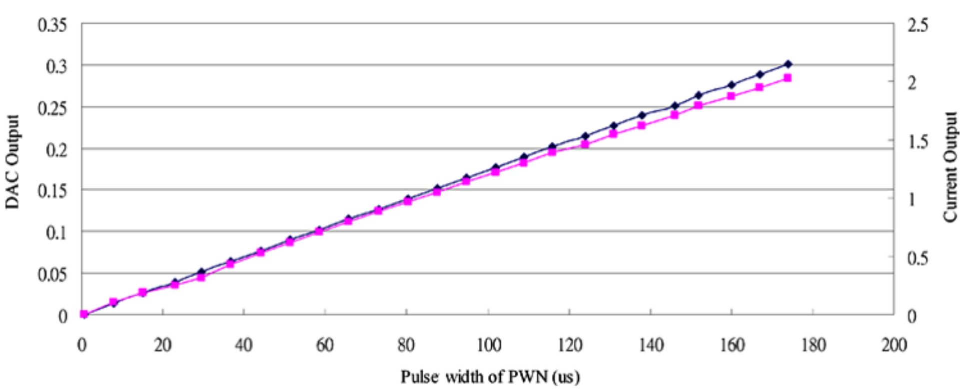

FIGURE 7 The relationships among pulse width of the PWM, DAC, and current.

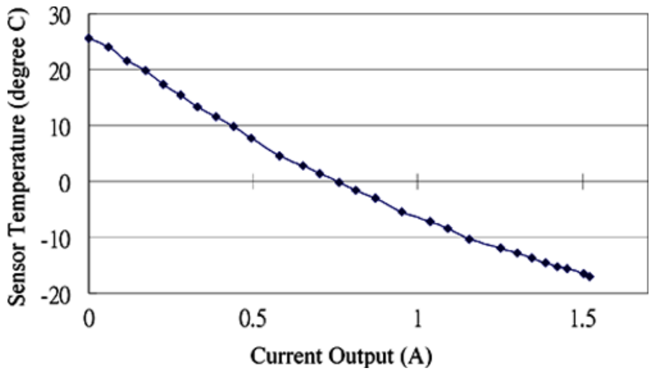

FIGURE 8 The relationship between current output and sensor temperature.

In Figure 8, the curve shows that the temperature of the image sensor can descend to −19°C and that the current of the TE cooling module needed to be about 1.6 A. In addition, we also tested the performance of the image sensor. Figure 9 shows the cooling temperature, integration time, and dark output state of the SWIR image sensor. The dark state outputs of the SWIR image sensor increased at higher temperatures. For example, the dark state output of the SWIR image sensor was reduced by 50% as soon as the sensor temperature changed from 30°C to 20°C. The variation of the dark state output of the SWIR image sensor with respect to temperature became more obvious with long integration times. The variance between 0°C and −20°C was only about 5 mV. Figure 10 shows the output signals of 50 different pixels under −20°C and 30°C at a 10 ms integration time period. These observed signals more severely fluctuated at 30°C (dotted line) than those at −20°C (solid line). The SNR data was also calculated

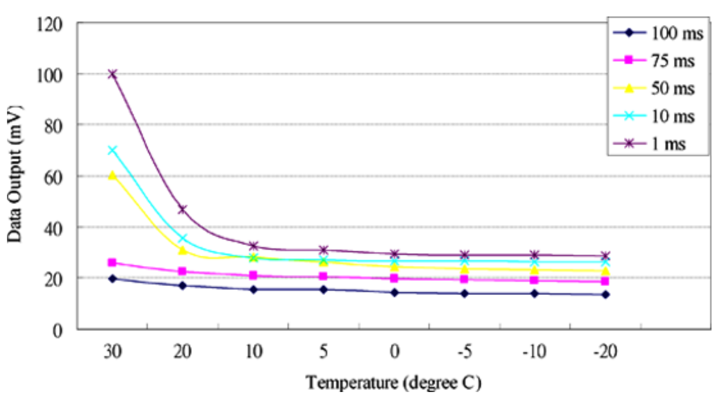

FIGURE 9 Output of the dark state during different integration times and the temperature.

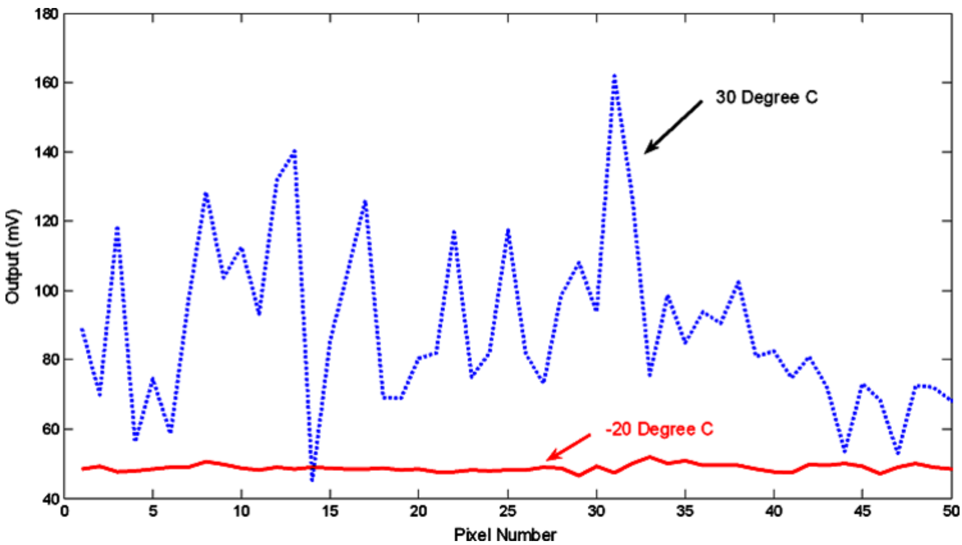

FIGURE 10 Output stability of one pixel at 30°C and at −20°C.

to display the performance of SWIR image sensor. The SNR is 48 dB in 30°C. It was improved to 84 dB in −20°C.

CONCLUSIONS

We demonstrated the effective cost, general purpose, and ease of integration of our new system with other measurement systems in this paper. A maximum 2 A current output can be automatically controlled by the PWM signal, which is modulated with temperature data. It provides a stable current proportional to the cooling device. The temperature measurement is crucial in the modification of the PWM signal. The thermistor type and voltage type thermal sensor were designed as outlined in this article. All of the system functioned in the dark output of the SWIR linear image sensor experiment. We also found that a short integration time and low temperature reduced the output of the dark state of the image sensor and increased the stability and SNR of the pixels of the image sensor.

REFERENCES

1. Rychen, J.; Ihn, T.; Studerus, P.; Heremann, A.; Ensslin, K. A low-temperature dynamic mode scanning force microscope operating in high magnetic fields. Rev. Sci. Inst. **1999**, *70*, 2765.
2. Labudovic, M.; Li, J. Modeling of TE cooling of pump lasers, Compon. Packag. IEEE Trans. **2004**, *27*, 724–730.
3. Taylor, R.A.; Solbrekken, G.L. Comprehensive system-level optimization of thermoelectric devices for electronic cooling applications, Compon. Packag. IEEE Trans. **2008**, *31*, 23–31.

4. Fukutani, K.; Shakouri, A. Design of bulk thermoelectric modules for integrated circuit thermal management, Compon. Packag. IEEE Trans. **2006**, *29*, 750–757.
5. Solbrekken, G.L.; Yazawa, K.; Bar-Cohen, A. Thermal management of portable electronic equipment using thermoelectric energy conversion, In Inter Society Conference on Thermal Phenomena, Proceeding of the Japan Conference, Tokyo, Juan 1–4, 2004.
6. Ahiska, R.; Ahiska, G.; Ahiska, K. Analysis of a new method for measurement of parameters of real thermoelectric module employed in medical cooler for renal hypothermia. Instrum. Sci. & Technol. **2009**, *37*, 102–123.
7. Ramirez, M.J.; Ortiz, A.J. U.S. Patent No. 5450727, 19 Sep 1995.
8. Thomas, M. U.S. Patent No. 5970719, 26 Oct 1999.
9. Parks, C.; Losee, D. Large-area interline CCD with low-dark current, In Sensors and Camera Systems for Scientific, Industrial, and Digital Photography Applications IV, Proceeding of the American Conference, Santa Clara, CA, USA, January 21, 2003.
10. ATmega8535 microcontroller. http://www.atmal.com
11. G9201-256S SWIR Image Sensor. http://www.hamamatsu.com/